# A Damage Model for Collagen Fibres with an Application to Collagenous Soft Tissues

Gerhard A. Holzapfel[1,2] and Ray W. Ogden[3]

[1]Institute of Biomechanics, Graz University of Technology
Stremayrgasse 16-II, 8010 Graz, Austria

[2]Norwegian University of Science and Technology (NTNU)
Faculty of Engineering Science and Technology, 7491 Trondheim, Norway

[3]School of Mathematics and Statistics, University of Glasgow
University Place, Glasgow G12 8SQ, Scotland, UK

To appear in the ***'Proc. R. Soc. Lond. A'***
March 20, 2020

**Abstract.** We propose a mechanical model to account for progressive damage in collagen fibres within fibrous soft tissues. The model has a similar basis to the pseudoelastic model that describes the Mullins effect in rubber but it also accounts for the effect of cross-links between collagen fibres. We show that the model is able to capture experimental data obtained from rat tail tendon fibres, and the combined effect of damage and collagen cross-links is illustrated for a simple shear test. The proposed three-dimensional framework allows a straightforward implementation in finite element codes which are needed to analyse more complex boundary-value problems for soft tissues under supra-physiological loading or tissues weakened by disease.

**Keywords:** Artery elasticity; collagen fibres; collagen cross-links; fibrous tissue; fibre damage

## 1 Introduction

Fibrous soft tissues consist of distributions of collagen fibres which, for example, could be almost parallel, as is the case for tendons, dispersed, as for artery walls, or isotropic, as for the middle zone of cartilage. These fibres are embedded in an essentially isotropic extrafibrillar matrix consisting of elastic fibres (including elastin), proteoglycans, water, adhesion proteins, and integrins, *inter alia.* Of particular interest are the mechanical properties of the collagen fibres, the main load bearing constituent of soft tissues, and their contribution to the overall behaviour of the tissues [1]. There are several constitutive models available that capture the distribution of collagen fibres [2–5]. However, it is important to note that under certain supra-physiological loads and in certain tissue diseases collagen starts to soften and finally ruptures, as shown by the experimental data in Pins and Silver [6] on a single collagen fibre. But as yet such effects

on the microscale have not been incorporated in constitutive models. For soft biological tissues a number of damage models are available, as described in the review article [7]. For example, the study [8] derives a fibre/fibril damage model based on failure once a critical tissue stretch is reached. The proposed model reproduces the typical nonlinear behaviour of ligaments including the toe and linear regions, then damage, and eventual failure. The computational work [9] proposes a (rather complex) macroscopic tissue damage model by considering recruitment stretches for the fibre content and failure of fibres in a distribution at different stretches or strain energies. Decoupled damage mechanisms for the matrix and fibres are considered. On the basis of [8] the constitutive model in [10] considers fibre recruitment and damage distributions by using probability density functions. It also includes a constitutive model for unloading after damage. The recent work [11] applies the constrained mixture theory of [12] to study the formation/dilatation of abdominal aortic aneurysms. In particular, the constitutive model accounts for continuous degradation and creation of collagen fibres (i.e. disappearance of old collagen and appearance of new collagen). The purpose of the present paper is now to develop a basic model at the collagen/cross-link microscale level that can account for these softening and failure effects.

The influence of the concentration of collagen fibre cross-links on the anisotropic response of fibrous soft tissues such as arterial walls was first analysed with a fully 3D model in [13]. However, that approach was solely based on the theory of hyperelasticity and no damage mechanism was included, which limits its applicability. Another aim of this paper is therefore to account for collagen fibre damage in the presence of undamaged cross-links which is the subject of §2. The model has a similar structure to that of the pseudoelastic model of the Mullins effect of rubber published in [14] but takes account of damage during loading rather than unloading. In the present account this damage model is used to reproduce the experimental behaviour of rat tail tendon fibres. In §3, with the inclusion of cross-links, we analyse the combined effect of damage and cross-links in the simple shear of a single family of parallel fibres embedded in an isotropic matrix. In particular, we demonstrate the influence of damage and the proportion of cross-links on the shear stress versus the amount of shear response. This illustrates that fibre damage leads to a softening behaviour and finally failure of the tissue. In §4 we provide concluding remarks and point to the needs for further experimental data on the microscopic level to inform the macroscopic tissue behaviour. This model approach can be implemented in a finite element code to execute more realistic boundary-value problems, for which purpose we provide the elasticity tensor in the appendix.

# 2 Damage model considering cross-linking

## 2.1 Damage formulation

We start by introducing the deformation gradient $\mathbf{F}$ relative to a given reference configuration, and the related right and left Cauchy–Green tensors $\mathbf{C} = \mathbf{F}^{\mathrm{T}}\mathbf{F}$ and $\mathbf{b} = \mathbf{F}\mathbf{F}^{\mathrm{T}}$, respectively. For further use we define the isotropic invariant $I_1$ and the pseudo-invariant $I_4$ according to

$$I_1 = \mathrm{tr}\mathbf{C}, \qquad I_4 = (\mathbf{C}\mathbf{M}) \cdot \mathbf{M} = \lambda^2, \tag{1}$$

where $\mathbf{M}$ is the direction of aligned fibres in the stress-free reference configuration which are embedded in an isotropic matrix, and $\lambda$ is the fibre stretch. Now let us consider a fibre-reinforced material such as a collagenous soft tissue, which is subject to the incompressibility constraint $\det\mathbf{F} = 1$, with the strain-energy function of the form $\Psi(I_1, I_4)$. The Cauchy stress tensor $\boldsymbol{\sigma}$ is then given by [15]

$$\boldsymbol{\sigma} = 2\psi_1\mathbf{b} + 2\psi_4\mathbf{m} \otimes \mathbf{m} - p\mathbf{I}, \tag{2}$$

where $p$ is a Lagrange multiplier, and $\mathbf{m} = \mathbf{F}\mathbf{M}$ is the fibre direction in the deformed configuration. Here, for convenience, we have introduced the abbreviations

$$\psi_1 = \frac{\partial\Psi}{\partial I_1}, \qquad \psi_4 = \frac{\partial\Psi}{\partial I_4}. \tag{3}$$

Now we consider the possibility of damage occurring when the stretch $\lambda$ in the fibre exceeds some critical value, say $\lambda_{\mathrm{c}}$. To model the damage effect we introduce a (dimensionless) damage variable $\eta$, which is an additional independent variable so that $\Psi(I_1, I_4, \eta)$. In the damage phase the Cauchy stress is again given by (2) with the optimization condition

$$\frac{\partial\Psi}{\partial\eta} = 0, \tag{4}$$

which gives $\eta$ implicitly in terms of $I_1$ and $I_4$. Let $I_{4\mathrm{c}} = \lambda_{\mathrm{c}}^2$ be the critical value of $I_4$. We take $\eta = 1$ whenever $I_4 \leq I_{4\mathrm{c}}$, so (2) applies with $\Psi(I_1, I_4, 1)$ and (4) is not active. For definiteness, we now take

$$\Psi(I_1, I_4, \eta) = \Psi_{\mathrm{iso}}(I_1) + \eta\Psi_{\mathrm{fib}}(I_4) + \phi(\eta), \tag{5}$$

analogously to the model of the Mullins effect [14], where $\phi(\eta)$ is some measure of damage. Then (2) gives

$$\boldsymbol{\sigma} = 2\psi_{\mathrm{i}}\mathbf{b} + 2\eta\psi_{\mathrm{f}}\mathbf{m} \otimes \mathbf{m} - p\mathbf{I}, \tag{6}$$

where we have introduced the abbreviations

$$\psi_{\mathrm{i}} = \frac{\partial\Psi_{\mathrm{iso}}}{\partial I_1}, \qquad \psi_{\mathrm{f}} = \frac{\partial\Psi_{\mathrm{fib}}}{\partial I_4}, \tag{7}$$

and with (5), the optimization condition (4) gives

$$\phi'(\eta) = -\Psi_{\rm fib}(I_4), \tag{8}$$

which determines $\eta$ in terms of $I_4$, i.e. damage is only related to the fibres. We require

$$\phi(1) = 0, \qquad \phi'(1) = -\Psi_{\rm fib}(I_{4\rm c}). \tag{9}$$

Note that if we use (4) to give $\eta = \eta(I_4)$ and write, say,

$$\overline{\Psi}(I_4) = \eta\Psi_{\rm fib}(I_4) + \phi(\eta), \tag{10}$$

then by (8) we obtain $\overline{\Psi}' = \eta\psi_{\rm f}$, where $\psi_{\rm f}$ is according to $(7)_2$. This leads to an alternative arrival at the second term on the right-hand side of (6).

A suitable choice of $\phi'(\eta)$, which gives a decaying behaviour for $\eta$ as $I_4$ increases beyond $I_{4\rm c}$ and damage progresses, is

$$\phi'(\eta) = m\log\eta - \Psi_{\rm fib}(I_{4\rm c}), \tag{11}$$

and hence, by (8),

$$\eta = \exp\left(-\frac{\Psi_{\rm fib}(I_4) - \Psi_{\rm fib}(I_{4\rm c})}{m}\right), \tag{12}$$

where $m > 0$ is a parameter with the same dimension as $\Psi$. Figure 1 provides a schematic of the damage parameter $\eta$ as a function of the stretch $\lambda$. It shows that $\eta$ decreases from $1$ when the stretch $\lambda$ increases beyond the critical value $\lambda_{\rm c}$ down to the value $\eta_{\rm f}$ when $\lambda$ reaches the failure value $\lambda_{\rm f}$. This schematic is based on specific calculations of $\eta$ for uniaxial extension and simple shear, which exhibit very similar behaviour.

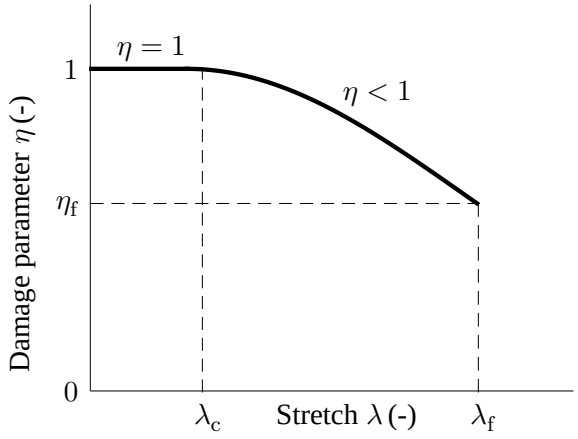


Figure 1: Damage parameter $\eta$ versus stretch $\lambda$, with critical stretch $\lambda_{\rm c}$ and failure stretch $\lambda_{\rm f}$.

## 2.2 Uniaxial extension

Let $\lambda$ be the stretch in the fibre direction $\mathbf{M}$ and $\sigma$ the related uniaxial Cauchy stress. Then, the components of (6) yield

$$\sigma = 2\psi_{\rm i}\lambda^2 + 2\eta\lambda^2\psi_{\rm f} - p, \qquad 0 = 2\psi_{\rm i}\lambda^{-1} - p, \tag{13}$$

and hence, on elimination of $p$,

$$\sigma = 2\psi_{\rm i}(\lambda^2 - \lambda^{-1}) + 2\eta\lambda^2\psi_{\rm f}, \tag{14}$$

where $\psi_{\rm i}$ and $\psi_{\rm f}$ are defined in (7). Now choose

$$\Psi_{\rm iso} = \frac{\mu}{2}(I_1 - 3), \qquad \Psi_{\rm fib} = \frac{k_1}{2k_2}\left\{\exp[k_2(I_4 - 1)^2] - 1\right\}, \tag{15}$$

for the matrix and the fibre properties, respectively, where $\mu$ and $k_1$ are stress-like parameters, while $k_2$ is dimensionless. Hence, according to (7), $2\psi_{\rm i} = \mu$ and $2\psi_{\rm f} = 2k_1(I_4 - 1)\exp[k_2(I_4 - 1)^2]$ so that (12) gives

$$\eta = \exp\left[-\frac{k_1}{2mk_2}\{\exp[k_2(I_4 - 1)^2] - \exp[k_2(I_{4\rm c} - 1)^2]\}\right], \tag{16}$$

with $I_4 = \lambda^2$ and $I_{4\rm c} = \lambda_{\rm c}^2$.

From (14) we then obtain

$$\sigma = \mu(\lambda^2 - \lambda^{-1}) + 2k_1\lambda^2(\lambda^2 - 1)\exp[k_2(\lambda^2 - 1)^2], \tag{17}$$

when no damage occurs ($\lambda \leq \lambda_{\rm c}$), and

$$\sigma = \mu(\lambda^2 - \lambda^{-1}) + 2\eta k_1\lambda^2(\lambda^2 - 1)\exp[k_2(\lambda^2 - 1)^2], \tag{18}$$

with (16), when $\lambda \geq \lambda_{\rm c}$.

The nominal stress $P = \sigma/\lambda$ is plotted in figure 2 as a fit to the uniaxial test data from a rat tail tendon fibre shown in [6], using the parameter values $\mu = 0$, $k_1 = 115\,$MPa, $k_2 = 7.7$, $m = 6\,$MPa, and $\lambda_{\rm c} = 1.05$. Note that since we are modelling a single fibre here we emphasize that there is no need to include the isotropic term.

From (11) and $(9)_1$, we have

$$\phi(\eta) = m\eta\log\eta + (1 - \eta)[m + \Psi_{\rm fib}(I_{4\rm c})], \tag{19}$$

and from (12)

$$m\log\eta = \Psi_{\rm fib}(I_{4\rm c}) - \Psi_{\rm fib}(I_4). \tag{20}$$

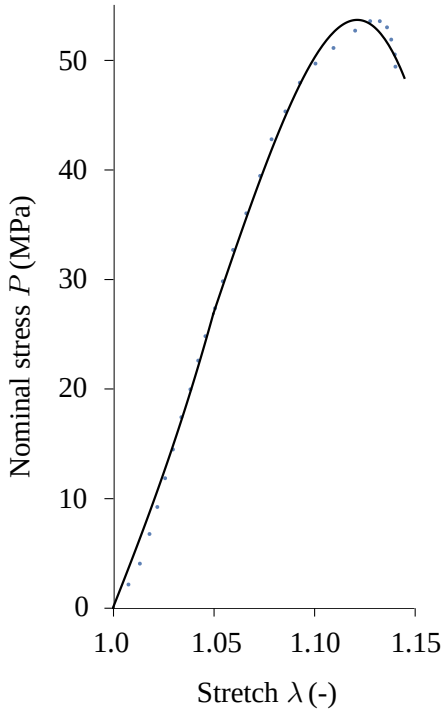


Figure 2: Fit to experimental data from rat tail tendon fibre taken from [6], whereby the dots represent the data extracted digitally from the curve in [6]. The solid curve shows the nominal stress $P = \sigma/\lambda$ versus stretch $\lambda$ according to (18) with $\mu = 0$ and $k_1 = 115\,\text{MPa}$, $k_2 = 7.7$, $m = 6\,\text{MPa}$, $\lambda_\text{c} = 1.05$.

There is no energy loss for $I_4 \leq I_{4\text{c}}$. Energy loss for $I_4 \geq I_{4\text{c}}$ is given by

$$\Psi_\text{fib} - [\eta\Psi_\text{fib} + \phi(\eta)] = m(\eta - \log\eta - 1) > 0 \qquad \text{for} \qquad \eta < 1. \tag{21}$$

Although there are no data available for the unloading phase it is worthwhile to illustrate the stress softening affect induced by $\eta$ during unloading prior to failure. For uniaxial extension this is shown by the schematic in Fig. 3 with three unloading curves from different points on the loading path. This parallels Fig. 2 with the nominal stress versus stretch.

## 2.3 Inclusion of collagen fibre cross-links

Let us use the unit vector **M**, which identifies the collagen fibre direction in the reference configuration, and introduce **N**, which is an arbitrary unit vector orthogonal to **M**. Now we consider two families of cross-links around the collagen fibre direction **M** with the unit vectors $\mathbf{L}^+$ and $\mathbf{L}^-$ which are rotationally symmetric about **M** and with the action of **F** on them defined by

$$\mathbf{L}^\pm = \pm\cos\alpha_0\mathbf{M} + \sin\alpha_0\mathbf{N}, \qquad \mathbf{F}\mathbf{L}^\pm = \pm c_0\mathbf{F}\mathbf{M} + s_0\mathbf{F}\mathbf{N}, \tag{22}$$

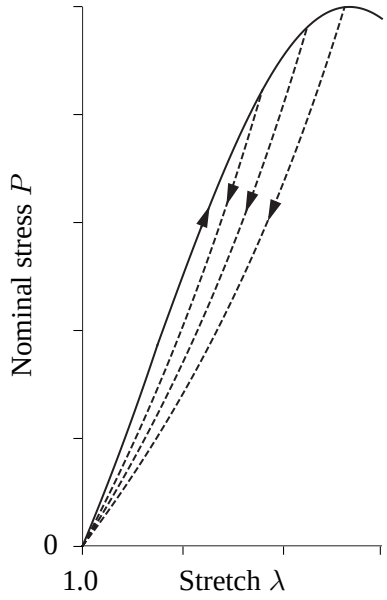


Figure 3: Schematic of the nominal stress $P$ versus stretch $\lambda$ during loading in uniaxial extension (continuous curve), with unloading curves (dashed) from three different points on the loading curve prior to failure.

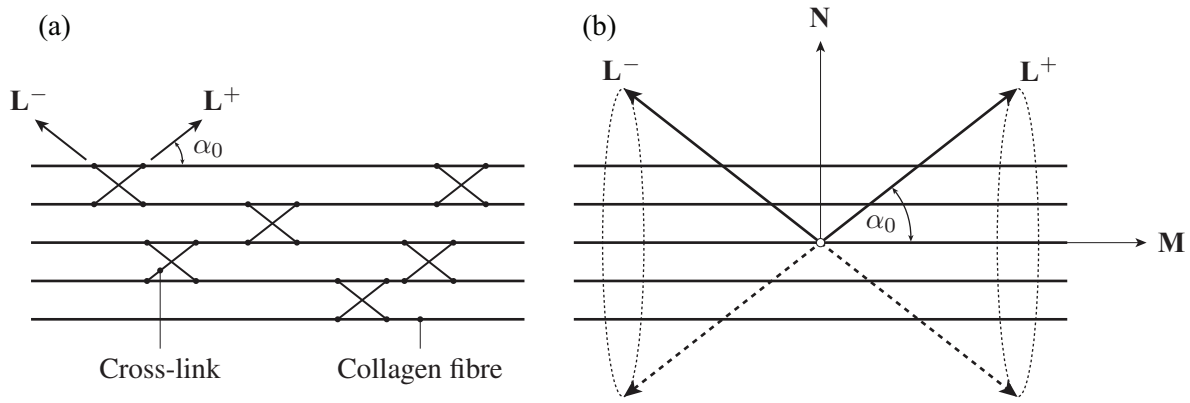


Figure 4: (a) Parallel fibres in the **M** direction with two families of parallel cross-links described by the vectors $\mathbf{L}^+$ and $\mathbf{L}^-$ making an angle $\alpha_0$ with **M**. (b) Detail of a pair of cross-links, showing rotational symmetry about the **M** direction with the orthogonal vector **N**; adopted from [13].

where $\alpha_0$ defines their orientation relative to the direction **M**; see Fig. 4. For conciseness we have written $s_0 = \sin\alpha_0$ and $c_0 = \cos\alpha_0$.

The invariant $I_4$ associated with the fibre direction is given in $(1)_2$, and the invariants $I^{\pm}$, which are the squares of the stretches in the cross-link directions, and the quantities $I_8^{\pm}$ describ-

ing the coupling between the collagen fibres and cross-links are defined by [13]

$$I^{\pm} = c_0^2 I_4 \pm 2 s_0 c_0 (\mathbf{CM}) \cdot \mathbf{N} + s_0^2 (\mathbf{CN}) \cdot \mathbf{N}, \qquad I_8^{\pm} = \pm c_0 I_4 + s_0 (\mathbf{CM}) \cdot \mathbf{N}. \tag{23}$$

Note that, in general, $I^+ \neq I^-$ and $I_8^+ \neq -I_8^-$.

From the derivatives of $I_4$, $I^{\pm}$ and $I_8^{\pm}$ with respect to the right Cauchy–Green tensor $\mathbf{C}$ given in [13] applied to a strain-energy function $\Psi(I_1, I_4, I^+, I^-, I_8^+, I_8^-)$ we obtain the general expression of the Cauchy stress tensor as

$$\begin{aligned}
\boldsymbol{\sigma} = & -p\mathbf{I} + 2\psi_1 \mathbf{b} + 2\psi_4 \mathbf{FM} \otimes \mathbf{FM} \\
& + 2\psi_{I^+}[c_0^2 \mathbf{FM} \otimes \mathbf{FM} + s_0 c_0 (\mathbf{FM} \otimes \mathbf{FN} + \mathbf{FN} \otimes \mathbf{FM}) + s_0^2 \mathbf{FN} \otimes \mathbf{FN}] \\
& + 2\psi_{I^-}[c_0^2 \mathbf{FM} \otimes \mathbf{FM} - s_0 c_0 (\mathbf{FM} \otimes \mathbf{FN} + \mathbf{FN} \otimes \mathbf{FM}) + s_0^2 \mathbf{FN} \otimes \mathbf{FN}] \\
& + \psi_{8^+}[2 c_0 \mathbf{FM} \otimes \mathbf{FM} + s_0 (\mathbf{FM} \otimes \mathbf{FN} + \mathbf{FN} \otimes \mathbf{FM})] \\
& + \psi_{8^-}[-2 c_0 \mathbf{FM} \otimes \mathbf{FM} + s_0 (\mathbf{FM} \otimes \mathbf{FN} + \mathbf{FN} \otimes \mathbf{FM})],
\end{aligned} \tag{24}$$

as in [13], but with a slightly different notation, where we have used the abbreviations

$$\psi_{I^{\pm}} = \frac{\partial \Psi}{\partial I^{\pm}}, \qquad \psi_{8^{\pm}} = \frac{\partial \Psi}{\partial I_8^{\pm}} \tag{25}$$

in addition to $\psi_1$ and $\psi_4$ defined in (3).

Note that the second Piola–Kirchhoff stress, which is important for finite element implementations, here denoted by $\mathbf{S}$, is related to $\boldsymbol{\sigma}$ by $\mathbf{S} = \mathbf{F}^{-1} \boldsymbol{\sigma} \mathbf{F}^{-\mathrm{T}}$ for an incompressible material. Consequently, we can determine the total differential

$$\mathrm{d}\mathbf{S} = \mathbb{C} : \frac{1}{2} \mathrm{d}\mathbf{C}, \tag{26}$$

where the colon denotes the standard double contraction, and $\mathbb{C}$ is the elasticity tensor in the material description required for finite element analysis. For a general explicit expression for $\mathbb{C}$ we refer to the appendix.

### 2.3.1 Uniaxial extension with cross-linking

For uniaxial extension with stretch $\lambda$ in the fibre direction we have

$$\mathbf{FM} = \lambda \mathbf{M}, \quad \mathbf{FN} = \lambda^{-1/2} \mathbf{N}. \tag{27}$$

Hence, with these two equations we can deduce from $(22)_2$

$$\mathbf{FL}^{\pm} = \pm c_0 \lambda \mathbf{M} + s_0 \lambda^{-1/2} \mathbf{N}, \tag{28}$$

and (23) specializes to

$$I \equiv I^{\pm} = c_0^2\lambda^2 + s_0^2\lambda^{-1}, \qquad I_8 = I_8^+ = c_0\lambda^2, \qquad I_8^- = -I_8^+. \tag{29}$$

Then $\psi_I = \psi_{I^+} = \psi_{I^-}, \psi_{8^+} = -\psi_{8^-} = \psi_8$, and (24) specializes to

$$\begin{aligned}\boldsymbol{\sigma} = &-p\mathbf{I} + 2\psi_1(\lambda^2\mathbf{M}\otimes\mathbf{M} + \lambda^{-1}\mathbf{N}\otimes\mathbf{N}) + 2\psi_4\lambda^2\mathbf{M}\otimes\mathbf{M}\\ &+4\psi_I(c_0^2\lambda^2\mathbf{M}\otimes\mathbf{M} + s_0^2\lambda^{-1}\mathbf{N}\otimes\mathbf{N}) + 4\psi_8 c_0\lambda^2\mathbf{M}\otimes\mathbf{M},\end{aligned} \tag{30}$$

the relevant components of which are

$$\sigma = -p + 2\psi_1\lambda^2 + 2\psi_4\lambda^2 + 4\psi_I c_0^2\lambda^2 + 4\psi_8 c_0\lambda^2, \tag{31}$$

$$0 = -p + 2\psi_1\lambda^{-1} + 4\psi_I s_0^2\lambda^{-1}. \tag{32}$$

By eliminating the Lagrange multiplier $p$ we obtain

$$\sigma = 2\psi_1(\lambda^2 - \lambda^{-1}) + 2\psi_4\lambda^2 + 4\psi_I(c_0^2\lambda^2 - s_0^2\lambda^{-1}) + 4\psi_8 c_0\lambda^2. \tag{33}$$

Now let us use the specific strain-energy functions (15) supplemented by quadratic energy functions associated with the cross-links and fibre/cross-link interactions so that

$$\Psi = \frac{1}{2}\mu(I_1 - 3) + \eta\frac{k_1}{2k_2}\{\exp[k_2(I_4 - 1)^2] - 1\} + \frac{1}{2}\nu(I-1)^2 + \frac{1}{2}\kappa(I_8 - c_0)^2, \tag{34}$$

where $\nu$ and $\kappa$ are parameters with dimension of stress associated with the cross-links and interactions, respectively. In particular, a larger $\nu$ corresponds to a larger density of cross-links, while $\kappa$ is a measure of the interaction energy. Here we have adopted very simple models for the energy in the cross-links and the interaction energy since there are no data available to justify more sophisticated forms of energy. From (12) with $(15)_2$, $\eta$ is given by

$$\eta = \exp\left[-\frac{k_1}{2mk_2}\left\{\exp[k_2(\lambda^2-1)^2] - \exp[k_2(\lambda_{\rm c}^2 - 1)^2]\right\}\right]. \tag{35}$$

From (33) and (34), with the help of (3) and (25), the Cauchy stress $\sigma$ then becomes

$$\begin{aligned}\sigma = &\mu(\lambda^2 - \lambda^{-1}) + 2k_1\eta\lambda^2(\lambda^2-1)\exp[k_2(\lambda^2-1)^2]\\ &+4\nu(I-1)(c_0^2\lambda^2 - s_0^2\lambda^{-1}) + 4\kappa(I_8 - c_0)c_0\lambda^2.\end{aligned} \tag{36}$$

The fit to the experimental data of [6] is of similar agreement to that shown in figure 2. Specific parameters are, e.g., $k_1 = 120\,$MPa, $\nu = 15\,$MPa, $k_2 = 6.4$, $m = 6\,$MPa, $\alpha_0 = \pi/4$, $\lambda_{\rm c} = 1.02$, $\kappa = 8\,$MPa and $\mu = 0$.

# 3 Application to planar deformation of soft tissues

Next we consider the situation in which the collagen fibres and cross-links are restricted to the ($\mathbf{E}_1$, $\mathbf{E}_2$) plane and we define by $\mathbf{M}$ the direction of the family of aligned fibres, and its normal $\mathbf{N}$ as

$$\mathbf{M} = \cos\alpha\mathbf{E}_1 + \sin\alpha\mathbf{E}_2, \quad \mathbf{N} = -\sin\alpha\mathbf{E}_1 + \cos\alpha\mathbf{E}_2, \tag{37}$$

where $\alpha$ is the angle between the fibre direction and the $\mathbf{E}_1$ axis (see figure 5). With respect

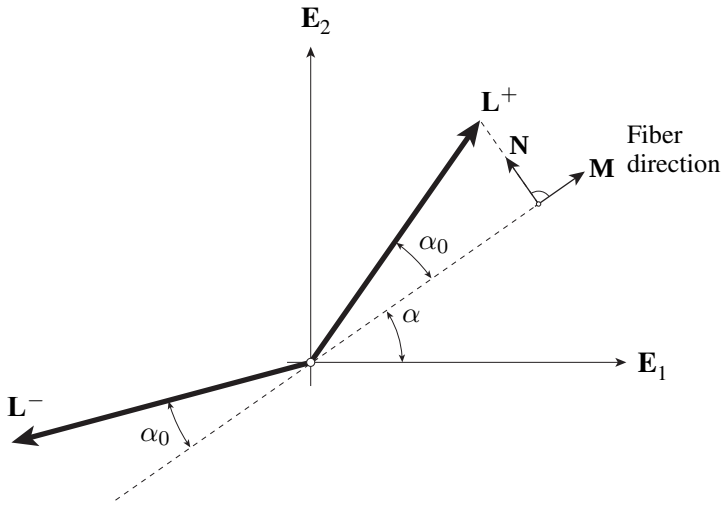


Figure 5: $\mathbf{M}$ represents the direction of a family of aligned fibres with unit normal $\mathbf{N}$ with respect to background axes $\mathbf{E}_1$ and $\mathbf{E}_2$, and $\mathbf{M}$ makes an angle $\alpha$ with respect to the $\mathbf{E}_1$ direction. $\mathbf{L}^{\pm}$ represent the directions of two families of cross-links, and $\mathbf{L}^{\pm}$ make an angle $\alpha_0$ with respect to the $\pm\mathbf{M}$ direction (modified from [13]).

to $\mathbf{M}$ and $\mathbf{N}$ the cross-link directions $\mathbf{L}^{\pm}$ between members of the family and the action of $\mathbf{F}$ thereon are again given by (22). The invariant $I_4 = (\mathbf{CM}) \cdot \mathbf{M}$, as in $(1)_2$, but with $\mathbf{M}$ now defined by $(37)_1$, while the invariants $I^{\pm}$ and the quantities $I_8^{\pm}$ are again given by (23). The Cauchy stress tensor $\boldsymbol{\sigma}$ has the same form (24) as in 3D but is now restricted to 2D.

## 3.1 Simple shear

For simple shear in the $\mathbf{E}_1$ direction in the considered plane, the deformation gradient is given by $\mathbf{F} = \mathbf{I} + \gamma\mathbf{E}_1 \otimes \mathbf{E}_2$, where $\gamma$ is the amount of shear. It follows that

$$\mathbf{FM} = \mathbf{M} + \gamma\sin\alpha\mathbf{E}_1, \qquad \mathbf{FN} = \mathbf{N} + \gamma\cos\alpha\mathbf{E}_1. \tag{38}$$

The invariant $I_4 = (\mathbf{CM}) \cdot \mathbf{M}$ is

$$I_4 = 1 + \gamma \sin 2\alpha + \gamma^2 \sin^2 \alpha, \tag{39}$$

while the required expressions $(\mathbf{CN}) \cdot \mathbf{N}$ and $(\mathbf{CM}) \cdot \mathbf{N}$ are given by

$$(\mathbf{CN}) \cdot \mathbf{N} = 1 - \gamma \sin 2\alpha + \gamma^2 \cos^2 \alpha, \quad (\mathbf{CM}) \cdot \mathbf{N} = \gamma \cos 2\alpha + \gamma^2 \sin \alpha \cos \alpha. \tag{40}$$

On substitution of (40) into (23) we obtain

$$I^{\pm} = 1 + \gamma \sin 2(\alpha \pm \alpha_0) + \gamma^2 \sin^2(\alpha \pm \alpha_0), \tag{41}$$

$$I_8^{\pm} = \pm c_0 + \gamma \sin(\alpha_0 \pm 2\alpha) + \gamma^2 \sin \alpha \sin(\alpha_0 \pm \alpha). \tag{42}$$

From (24) the components of the Cauchy stress can be obtained, but we only need here the shear component $\sigma_{12}$, i.e.

$$\begin{aligned} \sigma_{12} = {} & 2\psi_1 \gamma + 2[\psi_4 + c_0^2(\psi_{I^+} + \psi_{I^-}) + c_0(\psi_{8^+} - \psi_{8^-})]s(c + \gamma s) \\ & s_0[2c_0(\psi_{I^+} - \psi_{I^-}) + \psi_{8^+} + \psi_{8^-}](c^2 - s^2 + 2\gamma sc) \\ & + 2s_0^2(\psi_{I^+} + \psi_{I^-})c(\gamma c - s) \equiv \frac{\partial \Psi}{\partial \gamma}, \end{aligned} \tag{43}$$

where for conciseness we have written $s = \sin \alpha$ and $c = \cos \alpha$.

For illustrative purposes we now consider the model strain-energy function [13]

$$\begin{aligned} \Psi = {} & \frac{1}{2}\mu(I_1 - 3) + \eta \frac{k_1}{2k_2}\{\exp[k_2(I_4 - 1)^2] - 1\} + \frac{1}{2}\nu(I^+ - 1)^2 + \frac{1}{2}\nu(I^- - 1)^2 \\ & + \frac{1}{2}\kappa(I_8^+ - c_0)^2 + \frac{1}{2}\kappa(I_8^- + c_0)^2, \end{aligned} \tag{44}$$

which generalizes equation (34) to the case in which $I^+ \neq I^-$ and $I_8^+ \neq -I_8^-$. With (25) it follows that

$$\psi_{I^+} + \psi_{I^-} = 2\nu\gamma[2sc(c_0^2 - s_0^2) + \gamma(s_0^2 c^2 + s^2 c_0^2)], \tag{45}$$

$$\psi_{I^+} - \psi_{I^-} = 4\nu\gamma s_0 c_0(c^2 - s^2 + \gamma sc), \tag{46}$$

$$\psi_{8^+} + \psi_{8^-} = 2\kappa\gamma s_0(c^2 - s^2 + \gamma sc), \tag{47}$$

$$\psi_{8^+} - \psi_{8^-} = 2\kappa\gamma s c_0(2c + \gamma s). \tag{48}$$

In this case, from (12), we obtain, with the help of $(15)_2$ and (39),

$$\eta = \exp\left[-\frac{k_1}{2mk_2}\left\{\exp[k_2\gamma^2 s^2(\gamma s + 2c)^2] - \exp[k_2\gamma_{\mathrm{c}}^2 s^2(\gamma_{\mathrm{c}} s + 2c)^2]\right\}\right], \tag{49}$$

where $\gamma_{\mathrm{c}}$ is the critical value of $\gamma$ at which damage is initiated.

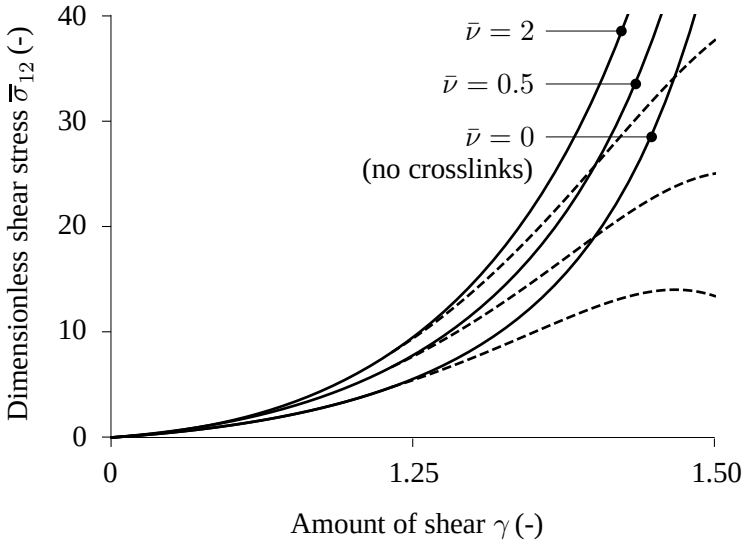


Figure 6: Plots of the dimensionless shear stress $\overline{\sigma}_{12}$ versus the amount of shear $\gamma$ with and without fibre damage (dashed and solid curves, respectively), with ($\bar{\nu} = \nu/\mu = 0.5, 2, \bar{\kappa} = \kappa/\mu = 0.6$) and without ($\bar{\nu} = \bar{\kappa} = 0$) cross-links. Parameter values: $\bar{k}_1 = k_1/\mu = 2$, $\alpha = \pi/3$, $k_2 = 0.1$, $\gamma_c = 0.7$, $m/\mu = 10$, $\alpha_0 = \pi/5$.

Hence, from (43), we obtain with (3) and (45)–(48)

$$\begin{aligned}\sigma_{12} = {} & \mu\gamma + 2\eta k_1 \exp[k_2\gamma^2 s^2(2c+\gamma s)^2]s^2(c+\gamma s)(2c+\gamma s)\gamma \\ & + 4\nu\gamma\{2s^2c^2(c_0^2-s_0^2)^2 + 2s_0^2c_0^2(c^2-s^2)^2 \\ & + 3sc\gamma[(c_0^2-s_0^2)(c_0^2s^2+s_0^2c^2) + 2s_0^2c_0^2(c^2-s^2)] + \gamma^2[(c_0^2s^2+s_0^2c^2)^2 + 4s_0^2c_0^2s^2c^2]\} \\ & + 2\kappa\gamma\{s_0^2 + 4s^2c^2(c_0^2-s_0^2) + 3sc\gamma[(s_0^2c^2+s^2c_0^2+s^2(c_0^2-s_0^2)] + 2\gamma^2s^2(s_0^2c^2+s^2c_0^2)\}.\end{aligned} \tag{50}$$

In figure 6 we plot the dimensionless shear stress $\bar{\sigma}_{12} = \sigma_{12}/\mu$ from (50) against the amount of shear $\gamma$ in order to illustrate the dependence on the various parameters. The specific parameter values used are $\bar{k}_1 = k_1/\mu = 2$, $\alpha = \pi/3$, $k_2 = 0.1$, $\gamma_c = 0.7$, $m/\mu = 10$, $\alpha_0 = \pi/5$, and $\bar{\nu} = \nu/\mu = 0.5, 2, \bar{\kappa} = \kappa/\mu = 0.6$. Without cross-links $\bar{\nu} = \bar{\kappa} = 0$. Clearly the shear stress response stiffens with an increase in the cross-link parameter $\bar{\nu}$ without damage, while when damage is included the shear stress is reduced after a critical value of $\gamma$ and can reach a maximum as $\gamma$ increases, as evidenced in the case when there are no cross-links. For the related elasticity tensor of model (44), which is relatively simple, we refer to the appendix.

# 4 Discussion and concluding remarks

This study proposes a simple mechanical model for the damage progression of stretched collagen fibres based on a pseudoelastic approach. The model is used to fit the limited data that is available on the stretching of an individual collagen fibre, and the agreement with the data is very satisfactory. The model has then been used for the construction of a constitutive model for fibre-reinforced soft tissues in which the collagen fibres are supported by cross-links. The predictions of the model have been illustrated by an application to a simple shear test in which both damage and cross-links are accounted for. The related elasticity tensor is also provided with a view to analyzing more complex boundary-value problems requiring a finite element implementation.

To inform the further development of models that incorporate damage and cross-linking more data are needed on the response and damage of stretched single fibres, their influence on aggregates of collagen fibres embedded in tissues and also the mechanical properties of the cross-links. It is well-known that the proportion of cross-links increases with age and causes a stiffening of the tissue [16]. In addition, several studies have shown that the stiffening of fibrous tissues is related to the concentration of cross-links; see, e.g., [17, 18]. Such a relationship is captured by our model.

The effect of proteoglycans is essentially incorporated into the isotropic part of the tissue model partly because it is still unclear what their mechanical contribution is to the overall response of the tissue. However, there is evidence that proteoglycans can support forces in the piconewton range when stretched [19] but it is not clear if the level of stresses they can support is relevant for a constitutive model of the type proposed in this paper. The review article by Scott [20] has described a mechanism between the collagen fibrils (as distinct from fibres) governed mainly by proteoglycans which are essentially orthogonal to the fibrils (note that the author calls this complex an ‘elastic shape module’). However, it seems that there is no quantification yet available that shows how the force is transmitted between the individual fibrils. In the present paper we focus on the collagen fibre level without accounting for the structure of fibrils and proteoglycans. In addition, because of the orthogonal arrangement of the proteoglycans with respect to the fibrils, see [21], the force transition would only be relevant for rather large deformations. It is worth pointing out, however, that force transition between proteoglycans and fibrils was accounted for in a mechanical model in [22], in which a collagen fibre is represented as a bundle of collagen fibrils cross-linked by proteoglycans.

More advanced multi-scale models are needed that capture the behaviours of the individual constituents such as proteoglycans, cross-linking proteins and their interaction with collagen

molecules, fibrils and fibres and their aggregated contributions to the tissue. There is hope that current imaging modalities will allow a better understanding of the structure down to the nanoscale, but there is also a need for mechanical information at the same level. In order to tackle organ level simulations the proposed model allows for a straightforward implementation within the finite element method, which is a powerful tool for analyzing more clinically relevant problems in health and disease.


## Acknowledgments

The work of G.A.H. was partly supported by the Lead Project on 'Mechanics, Modeling and Simulation of Aortic Dissection', granted by Graz University of Technology, Austria. The work of R.W.O. was in part funded by the UK EPSRC grant no. EP/N014642/1.


## Authors contributions

G.A.H. and R.W.O. conceived and designed the research, interpreted the results and drafted the manuscript. Both authors edited and revised the manuscript, and gave final approval for publication.

# Appendix

Here we explicitly present the elasticity tensor $\mathbb{C}$ in the material description which is defined by

$$\mathbb{C} = 4\frac{\partial^2 \Psi}{\partial \mathbf{C} \partial \mathbf{C}}. \tag{51}$$

Consider an energy function of the form $\Psi(I_1, I_4, I^{\pm}, I_8^{\pm}, \eta)$, where the four invariants are defined according to (1) and (23), $\eta = \eta(I_4)$ is a damage variable accommodating damage only in the fibres, which is not specified explicitly at this point, and where $I_4$ is the square of the stretch in the fibre direction. Then the derivatives of the invariants and $\eta$ with respect to $\mathbf{C}$ are

$$\frac{\partial I_1}{\partial \mathbf{C}} = \mathbf{I}, \quad \frac{\partial I_4}{\partial \mathbf{C}} = \mathbf{A}_{\mathrm{M}}, \quad \frac{\partial I^{\pm}}{\partial \mathbf{C}} = c_0^2 \mathbf{A}_{\mathrm{M}} \pm 2 s_0 c_0 \mathbf{A}_{\mathrm{MN}} + s_0^2 \mathbf{A}_{\mathrm{N}}, \quad \frac{\partial I_8^{\pm}}{\partial \mathbf{C}} = \pm c_0 \mathbf{A}_{\mathrm{M}} + s_0 \mathbf{A}_{\mathrm{MN}},$$

and

$$\frac{\partial \eta}{\partial \mathbf{C}} = \eta'(I_4) \mathbf{A}_{\mathrm{M}},$$

where we have introduced the notations

$$\mathbf{A}_{\mathrm{M}} = \mathbf{M} \otimes \mathbf{M}, \quad \mathbf{A}_{\mathrm{MN}} = \frac{1}{2}(\mathbf{M} \otimes \mathbf{N} + \mathbf{N} \otimes \mathbf{M}) = \mathbf{A}_{\mathrm{NM}}, \quad \mathbf{A}_{\mathrm{N}} = \mathbf{N} \otimes \mathbf{N}.$$

It follows that

$$\frac{\partial\Psi}{\partial\mathbf{C}} = \psi_1\mathbf{I} + [\psi_4 + c_0^2(\psi_{I^+} + \psi_{I^-}) + c_0(\psi_{I_8^+} - \psi_{I_8^-}) + \psi_\eta\eta']\mathbf{A}_{\rm M} \\ +[2s_0c_0(\psi_{I^+} - \psi_{I^-}) + s_0(\psi_{I_8^+} + \psi_{I_8^-})]\mathbf{A}_{\rm MN} + s_0^2(\psi_{I^+} + \psi_{I^-})\mathbf{A}_{\rm N},$$

where we have used the abbreviations (3), (25) and $\psi_\eta = \partial\Psi/\partial\eta$. Then, we can write

$$\frac{\partial^2\Psi}{\partial\mathbf{C}\partial\mathbf{C}} = a_1\mathbf{I}\otimes\mathbf{I} + a_2(\mathbf{I}\otimes\mathbf{A}_{\rm M} + \mathbf{A}_{\rm M}\otimes\mathbf{I}) + a_3\mathbf{A}_{\rm M}\otimes\mathbf{A}_{\rm M} + a_4(\mathbf{I}\otimes\mathbf{A}_{\rm N} + \mathbf{A}_{\rm N}\otimes\mathbf{I}) \\ +a_5(\mathbf{I}\otimes\mathbf{A}_{\rm MN} + \mathbf{A}_{\rm MN}\otimes\mathbf{I}) + a_6(\mathbf{A}_{\rm M}\otimes\mathbf{A}_{\rm N} + \mathbf{A}_{\rm N}\otimes\mathbf{A}_{\rm M}) + a_7\mathbf{A}_{\rm N}\otimes\mathbf{A}_{\rm N} \\ +a_8(\mathbf{A}_{\rm M}\otimes\mathbf{A}_{\rm MN} + \mathbf{A}_{\rm MN}\otimes\mathbf{A}_{\rm M}) + a_9(\mathbf{A}_{\rm N}\otimes\mathbf{A}_{\rm MN} + \mathbf{A}_{\rm MN}\otimes\mathbf{A}_{\rm N}) + a_{10}\mathbf{A}_{\rm MN}\otimes\mathbf{A}_{\rm MN},$$

where

$$a_1 = \psi_{11}, \quad a_2 = \psi_{14} + \psi_{1\eta}\eta' + c_0^2(\psi_{1I^+} + \psi_{1I^-}) + c_0(\psi_{1I_8^+} - \psi_{1I_8^-}),$$
$$a_3 = \psi_{44} + 2\psi_{4\eta}\eta' + \psi_{\eta\eta}\eta'^2 + \psi_\eta\eta'' + 2c_0^2[\psi_{4I^+} + \psi_{4I^-} + \eta'(\psi_{\eta I^+} + \psi_{\eta I^-})] \\ +2c_0[\psi_{4I_8^+} - \psi_{4I_8^-} + \eta'(\psi_{\eta I_8^+} - \psi_{\eta I_8^-})] + c_0^4(\psi_{I^+I^+} + \psi_{I^-I^-} + 2\psi_{I^+I^-}) \\ +c_0^2(\psi_{I_8^+I_8^+} + \psi_{I_8^-I_8^-} - 2\psi_{I_8^+I_8^-}) + 2c_0^3(\psi_{I^+I_8^+} - \psi_{I^+I_8^-} + \psi_{I^-I_8^+} - \psi_{I^-I_8^-}),$$
$$a_4 = s_0^2(\psi_{1I^+} + \psi_{1I^-}), \quad a_5 = 2s_0c_0(\psi_{1I^+} - \psi_{1I^-}) + s_0(\psi_{1I_8^+} + \psi_{1I_8^-}),$$
$$a_6 = s_0^2[\psi_{4I^+} + \psi_{4I^-} + \eta'(\psi_{\eta I^+} + \psi_{\eta I^-})] + s_0^2c_0^2(\psi_{I^+I^+} + \psi_{I^-I^-} + 2\psi_{I^+I^-}) \\ s_0^2c_0(\psi_{I^+I_8^+} - \psi_{I^+I_8^-} + \psi_{I^-I_8^+} - \psi_{I^-I_8^-}),$$
$$a_7 = s_0^4(\psi_{I^+I^+} + \psi_{I^-I^-} + 2\psi_{I^+I^-}),$$
$$a_8 = 2s_0c_0[\psi_{4I^+} - \psi_{4I^-} + \eta'(\psi_{\eta I^+} - \psi_{\eta I^-})] + s_0[\psi_{4I_8^+} + \psi_{4I_8^-} + \eta'(\psi_{\eta I_8^+} + \psi_{\eta I_8^-})] \\ +2s_0c_0^3(\psi_{I^+I^+} - \psi_{I^-I^-}) + s_0c_0(\psi_{I_8^+I_8^+} - \psi_{I_8^-I_8^-}) \\ +s_0c_0^2(3\psi_{I^+I_8^+} - \psi_{I^+I_8^-} - \psi_{I^-I_8^+} + 3\psi_{I^-I_8^-}),$$
$$a_9 = 2s_0^3c_0(\psi_{I^+I^+} - \psi_{I^-I^-}) + s_0^3(\psi_{I^+I_8^+} + \psi_{I^+I_8^-} + \psi_{I^-I_8^+} + \psi_{I^-I_8^-}),$$
$$a_{10} = 4s_0^2c_0^2(\psi_{I^+I^+} + \psi_{I^-I^-} - 2\psi_{I^+I^-}) + s_0^2(\psi_{I_8^+I_8^+} + \psi_{I_8^-I_8^-} + 2\psi_{I_8^+I_8^-}) \\ +4s_0^2c_0(\psi_{I^+I_8^+} + \psi_{I^+I_8^-} - \psi_{I^-I_8^+} - \psi_{I^-I_8^-}).$$

For notational simplicity the subscripts 1, 4, $8^+$ and $8^-$ on $\psi$ stand for $I_1$, $I_4$, $I_8^+$ and $I_8^-$, respectively, and we have introduced the abbreviation $\psi_{\bullet\star} = \partial^2\Psi/\partial(\bullet)\partial(\star)$. Note that in the expression for $a_2$ in eq. (78) of [13] the sign before $\psi_{1I_8^-}$ was incorrectly written as $+$.

For the model (44) these expressions simplify considerably, giving

$$a_1 = a_2 = a_4 = a_5 = a_8 = a_9 = 0,$$

$$a_3 = \eta(\psi_{\rm ff} - \psi_{\rm f}^2/m) + 2\nu c_0^4 + 2\kappa c_0^2, \quad a_6 = 2\nu s_0^2c_0^2, \quad a_7 = 2\nu s_0^4, \quad a_{10} = 8\nu s_0^2c_0^2 + 2\kappa s_0^2,$$

where $\psi_{\rm f}$ is defined according to $(7)_2$ and $\psi_{\rm ff} = \partial^2\Psi_{\rm fib}/\partial I_4^2$. Note that the explicit expressions for $\eta$ and $\Psi_{\rm fib}$ are provided in (12) and $(15)_2$, respectively.

# References


[1] P. Fratzl, editor. *Collagen. Structure and Mechanics*. Springer, New York, 2008.

[2] G. A. Holzapfel and R. W. Ogden. Constitutive modelling of arteries. *Proc. R. Soc. Lond. A*, 466:1551–1597, 2010.

[3] G. A. Holzapfel and R. W. Ogden. On the tension–compression switch in soft fibrous solids. *Eur. J. Mech. A/Solids*, 49:561–569, 2015.

[4] G. A. Holzapfel and R. W. Ogden. Biomechanical relevance of the microstructure in artery walls with a focus on passive and active components. *Am. J. Physiol. Heart Circ. Physiol.*, 315:H540–H549, 2018.

[5] G. A. Holzapfel, R. W. Ogden, and S. Sherifova. On fibre dispersion modelling of soft biological tissues: a review. *Proc. R. Soc. Lond. A*, 475:20180736, 2019.

[6] G. D. Pins and F. H. Silver. A self-assembled collagen scaffold suitable for use in soft and hard tissue replacement. *Mater. Sci. Eng. C*, 3:101–107, 1995.

[7] G. A. Holzapfel and B. Fereidoonnezhad. Modeling of damage in soft biological tissues. In Y. Payan and J. Ohayon, editors, *Biomechanics of Living Organs. Hyperelastic Constitutive Laws for Finite Element Modeling*, pages 101–123. Academic Press, 2017.

[8] C. Hurschler, B. Loitz-Ramage, and R. Vanderby Jr. A structurally based stress-stretch relationship for tendon and ligament. *J. Biomech. Eng.*, 119:392–399, 1997.

[9] V. Alastrué, J. F. Rodríguez, B. Calvo, and M. Doblaré. Structural damage models for fibrous biological soft tissues. *Int. J. Solids Structures*, 44:5894–5911, 2007.

[10] A. Hamedzadeh, T. C. Gasser, and S. Federico. On the constitutive modelling of recruitment and damage of collagen fibres in soft biological tissues. *Eur. J. Mech. A/Solids*, 72:483–496, 2018.

[11] W. J. Lin, M. D. Iafrati, R. A. Peattie, and L. Dorfmann. Growth and remodeling with application to abdominal aortic aneurysms. *J. Engr. Math.*, 109:113–137, 2018.

[12] J. D. Humphrey and K. R. Rajagopal. A constrained mixture model for growth and remodeling of soft tissues. *Math. Model. Meth. Appl. Sci.*, 12:407–430, 2002.

[13] G. A. Holzapfel and R. W. Ogden. An arterial constitutive model accounting for collagen content and cross-linking. *J. Mech. Phys. Solids*, 136:103682, 2020.

[14] R. W. Ogden and D. G. Roxburgh. A pseudo-elastic model for the Mullins effect in filled rubber. *Proc. R. Soc. Lond. A*, 455:2861–2877, 1999.

[15] G. A. Holzapfel. *Nonlinear Solid Mechanics. A Continuum Approach for Engineering*. John Wiley & Sons, Chichester, 2000.

[16] A. Tsamis, J. T. Krawiec, and D. A. Vorp. Elastin and collagen fibre microstructure of the human aorta in ageing and disease: a review. *J. R. Soc. Interface*, 10:20121004, 2013.

[17] V. M. Barodka, B. L. Joshi, D. E. Berkowitz, C. W. Hogue Jr., and D. Nyhan. Review article: implications of vascular aging. *Anesth. Analg.*, 112:1048–1060, 2011.

[18] C. Cantini, P. Kieffer, B. Corman, P. Limiñana, J. Atkinson, and I. Lartaud-Idjouadiene. Aminoguanidine and aortic wall mechanics, structure, and composition in aged rats. *Hypertension*, 38:943–948, 2001.

[19] R. G. Haverkamp, M. A. Williams, and J. E. Scott. Stretching single molecules of connective tissue glycans to characterize their shape-maintaining elasticity. *Biomacromolecules*, 6:1816–1818, 2005.

[20] J. E. Scott. Elasticity in extracellular matrix 'shape modules' of tendon, cartilage, etc. a sliding proteoglycan-filament model. *J. Physiol.*, 553:335–343, 2003.

[21] J. E. Scott. Cartilage is held together by elastic glycan strings. physiological and pathological implications. *Biorheology*, 45:209–217, 2008.

[22] T. C. Gasser. An irreversible constitutive model for fibrous soft biological tissue: a 3-D microfiber approach with demonstrative application to abdominal aortic aneurysms. *Acta Biomater.*, 7:2457–2466, 2011.